2010

Magnetic properties of Bi2FeMnO6: a multiferroic material with double-perovskite structure

Yi Du
University of Wollongong, ydu@uow.edu.au

Zhenxiang Cheng
University of Wollongong, cheng@uow.edu.au

S X. Dou
University of Wollongong, shi@uow.edu.au

Xiaolin Wang
University of Wollongong, xiaolin@uow.edu.au

Hua Zhao
National Institute For Materials Science, hz739@uow.edu.au

See next page for additional authors

Publication Details

Du, Y, Cheng, ZX, Dou, SX, Wang, XL, Zhao, HY & Kimura, H (2010), Magnetic properties of Bi2FeMnO6: a multiferroic material with double-perovskite structure, Applied Physics Letters, 97(12), pp. 1-3.

Magnetic properties of Bi2FeMnO6: a multiferroic material with double-perovskite structure

Abstract
Single phase Bi_2FeMnO_6 was synthesized on Si substrates by an electrospray method. Three peaks were observed in the temperature dependence of magnetization curve, which is attributed to the inhomogeneous distribution of Fe^{3+} and Mn^{3+}. The observed magnetic peaks at 150 K, 260 K, and 440 K correspond to orderings of the ferrimagnetic Fe–O–Mn, and antiferromagnetic Mn–O–Mn and Fe–O–Fe, respectively. Heat capacity measurements were carried out to confirm these magnetic transitions. The Debye temperature of Bi_2FeMnO_6 is 339 K, calculated from Debye–Einstein fitting.

Keywords
Magnetic, properties, Bi2FeMnO6, multiferroic, material, double, perovskite, structure

Disciplines
Engineering | Physical Sciences and Mathematics

Publication Details
Du, Y, Cheng, ZX, Dou, SX, Wang, XL, Zhao, HY & Kimura, H (2010), Magnetic properties of Bi2FeMnO6: a multiferroic material with double-perovskite structure, Applied Physics Letters, 97(12), pp. 1-3.

Authors
Yi Du, Zhenxiang Cheng, S X. Dou, Xiaolin Wang, Hua Zhao, and Hideo Kimura

Magnetic properties of Bi_2FeMnO_6: A multiferroic material with double-perovskite structure

Y. Du,[1] Z. X. Cheng,[1,a)] S. X. Dou,[1] X. L. Wang,[1,a)] H. Y. Zhao,[2] and H. Kimura[2]
[1]*Innovation Campus-AIIM Facility, Institute for Superconducting and Electronic Materials (ISEM), University of Wollongong, Squires Way, Fairy Meadow, New South Wales 2519, Australia*
[2]*National Institute for Materials Science, Sengen 1-2-1, Tsukuba, Japan*

(Received 25 May 2010; accepted 17 August 2010; published online 21 September 2010)

Single phase Bi_2FeMnO_6 was synthesized on Si substrates by an electrospray method. Three peaks were observed in the temperature dependence of magnetization curve, which is attributed to the inhomogeneous distribution of Fe^{3+} and Mn^{3+}. The observed magnetic peaks at 150 K, 260 K, and 440 K correspond to orderings of the ferrimagnetic Fe–O–Mn, and antiferromagnetic Mn–O–Mn and Fe–O–Fe, respectively. Heat capacity measurements were carried out to confirm these magnetic transitions. The Debye temperature of Bi_2FeMnO_6 is 339 K, calculated from Debye–Einstein fitting. © *2010 American Institute of Physics*. [doi:10.1063/1.3490221]

Multiferroic materials which display coexistence of ferromagnetism (FM) and ferroelectric (FE) polarization have drawn considerable attention due to their fundamental physical characteristics and potentially wide applications.[1–4] Unfortunately, candidate multiferroic materials are very rare due to the mutual exclusivity of the origins of FM and electric polarization, in which FM needs transition metals with unpaired 3*d* electrons and unfilled 3*d* orbital, while FE polarization needs transition metals with filled 3*d* orbital. Furthermore, the available multiferroic candidates, such as $BiFeO_3$,[5–9] $BiMnO_3$,[10–12] and $DyFeO_3$,[13] all have serious drawbacks, i.e., electric leakage or low temperature for appearance of multiferroic properties. Therefore, efforts to explore new candidate multiferroic materials are still highly desirable. Recently, a multiferroic material with double-perovskite structure, Bi_2FeMnO_6, has been theoretically designed.[14] It is expected that this material would show simultaneous magnetic ordering and electric polarization because it contains Bi^{3+} ions with unique $6s^2$ lone-pair electrons, similar to the examples of other bismuth transition metal oxides with simple perovskite structure. However, only a few studies on this compound have been reported, possibly due to the difficulties in the fabrication of this metastable material through a conventional high temperature synthesis process.[14] Therefore, reports on the detailed physical properties of this material have been awaited with great interest. In previous work,[15] room temperature multiferroic properties were reported for Nd:$BiFeO_3$/Bi_2FeMnO_6 bilayer films fabricated by the pulsed laser deposition method, and FM and FE properties were observed. However, due to the appearance of $BiFeO_3$, it is hard to subtract the intrinsic magnetic properties of Bi_2FeMnO_6. In this study, pure Bi_2FeMnO_6 samples were fabricated by an electrospray method. Its intrinsic magnetic properties have been observed.

Stoichiometric $Bi(NO_3)_3 \cdot 5H_2O$ and $Fe(NO_3)_3 \cdot 9H_2O$, and NH_4OH were dissolved in 2-methoxyethanol, forming dark brown 0.005 M precursor. Bi_2FeMnO_6 film was synthesized on a silicon substrate (heated up to 973 K) by an electrospray method in a high voltage field (20 kV) over 2 h. After that, the sample was sintered at 1173 K for 1 h. The sample was characterized by x-ray diffraction (XRD), XRD Rietveld refinement, scanning electron microscopy (SEM) equipped with energy dispersive spectroscopy (EDS). $B(B')$-site ion valence states were identified on an x-ray photoelectron spectrometer (XPS). Magnetic and thermal properties were measured by a 14T physical property measurement system (14T PPMS, Quantum Design) from 2 to 750 K in magnetic field up to 10 kOe.

Figure 1(a) shows the XRD pattern and refinement calculation results for Bi_2FeMnO_6. The XRD pattern of substrate has also been plotted in the figure. The sample is a well-crystallized single-phase film. Bi_2FeMnO_6 is a meta-

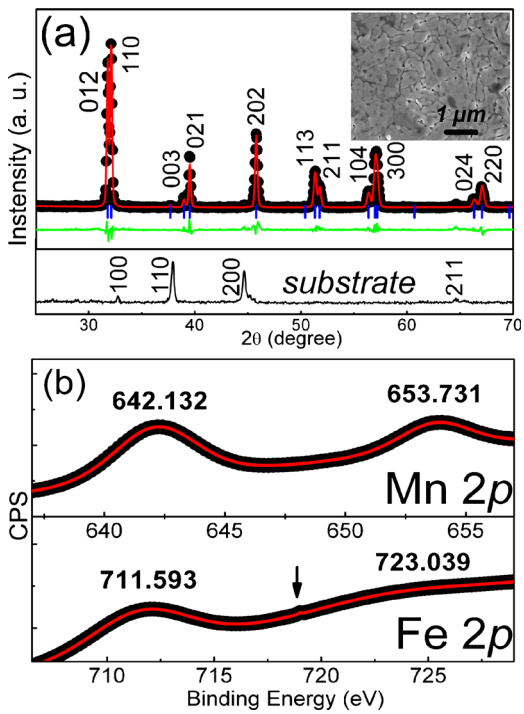

FIG. 1. (Color online) (a) XRD refinement calculation result for as-prepared Bi_2FeMnO_6 (R factors: R_P=8.1%, R_{WP}=10.7%). The XRD pattern of the substrate has been plotted as a reference. The inset is the SEM image for double-perovskite Bi_2FeMnO_6 film. (b) XPS spectra of the Fe 2*p* peaks and the Mn 2*p* peaks for Bi_2FeMnO_6 film.

a)Authors to whom correspondence should be addressed. Electronic addresses: xiaolin@uow.edu.au and cheng@uow.edu.au.

stable compound due to the positive formation enthalpy, as determined by first principles calculations.[14] It has been reported that its crystal structure varies from the $Pm\bar{3}m$, to the $R3c$, to the $C2$ space group, depending on the fabrication conditions. In this work, each of these structures has been adopted to refine the as-obtained XRD pattern. It was found that all the diffraction peaks except peaks from substrate can be indexed by using space group $R3c$ and a reliable refinement result could be achieved in contrast to the unreasonable deviations for refinement based on $Pm\bar{3}m$ and $C2$ groups. The refinement results show that Bi_2FeMnO_6 has a unit cell with lattice parameters $a=5.2575$ Å, $b=5.2575$ Å, and $c=13.072$ Å. The FeO_6 and MnO_6 polyhedra are elongated in the out-of-plane direction (c axis). The SEM image [Fig. 1(a) inset] indicates that the as-obtained sample is a polycrystalline granular film over the substrate. The thickness of film is around 550 nm. EDS spectra confirm the presence of the constituent elements in the sample with a ratio of ~1.97:1:1 in the order of Bi, Fe, and Mn, which is very close to the stoichiometry of Bi_2FeMnO_6. The slight deficiency of the bismuth will possibly lead to oxygen deficiency in order to keep charge balance in the compound which is very common for perovskite oxides, instead of formation of impurity phase which has been excluded by XRD result. It is difficult to have a conclusion of element distribution from EDS mapping results because the atomic distribution of Mn and Fe is out of the ability of EDS. In the stoichiometric Bi_2FeMnO_6, the average valence state of the $B(B')$-site cations is +3. Mn tends to exhibit multiple valences in many compounds with distorted perovskite structure,[16–18] which results in nonstoichiometric oxygen content and also reversely is a result of oxygen deficiency. In order to determine the valences of Mn and Fe ions in our sample, XPS measurements have been carried out, as shown in Fig. 1(b). In Mn $2p$ XPS result, only two main peaks of the $2p1/2$ (653.731 eV) and $2p3/2$ (642.132 eV), which are corresponding to Mn^{3+} ions, have been observed. It is known that the Fe $2p$ photoelectron peaks ($2p1/2$ at 723.0389 eV and $2p3/2$ at 711.593 eV) from oxidized iron are associated with satellite peaks, which is important for identifying the chemical states. The satellite peak was found 8 eV above the $2p3/2$ principal peak, in Bi_2FeMnO_6, which indicates the valence of Fe ions is +3. These results confirm that Mn and Fe ions in Bi_2FeMnO_6 film only present valence of +3.

Figure 2(a) displays the temperature dependence of the zero-field-cooled and field-cooled magnetic susceptibility $\chi(T)$, measured in a magnetic field of $H=1000$ Oe from 5 to 750 K for Bi_2FeMnO_6. From high temperature to low temperature, three magnetic peaks were observed, at 440 K (T_1), 260 K (T_2), and 150 K (T_3). Curie–Weiss fitting of the $1/\chi-T$ curve from 500 to 750 K, when the sample is in a paramagnetic state, was carried out as shown in the inset. The effective moment (μ_{eff}) on the $B(B')$-site was calculated to be $\mu_{eff}=7.5\ \mu_B$, where μ_B is the Bohr magneton. This result indicates that both Fe^{3+} and Mn^{3+} present high spin state (*HS*, $t_{2g}^3e_g^2$ for Fe^{3+} and $t_{2g}^3e_g^1$ for Mn^{3+}) electron configurations. The very high Curie–Weiss temperature, $\theta_P=-1020$ K indicates that Bi_2FeMnO_6 undergoes a strong antiferromagnetic (AFM) transition at T_1. According to the Goodenough–Kanamori rules for 180° superexchange coupling,[19] dissimilar ions of $Fe^{3+}-Mn^{3+}$ with both ions in the high spin state with a half-filled e_g orbital and one empty

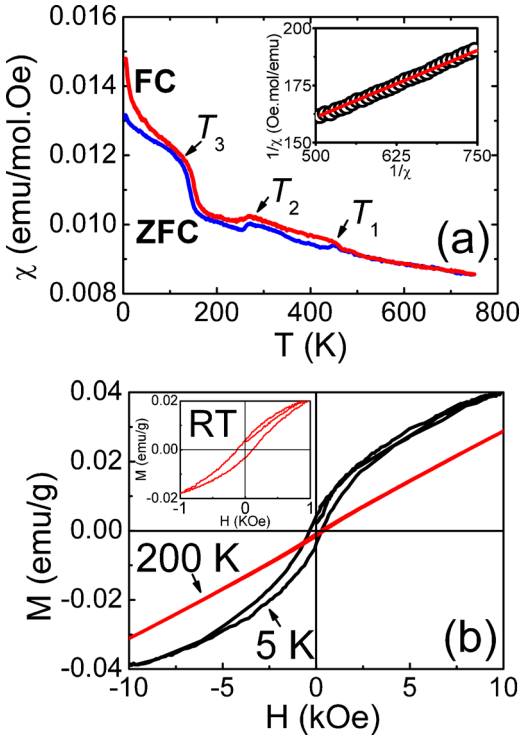

FIG. 2. (Color online) (a) Magnetization as a function of temperature ($5\ K<T<750\ K$); the solid line in the inset is the Curie–Weiss fitting for the M-T curve from 500 to 750 K. (b) Magnetization as a function of magnetic field at different temperatures; the inset is the M-H hysteresis loop observed at room temperature. The magnetic contribution from the substrate has been subtracted from all the data.

e_g orbital, most likely will result in antiparallel spin ordering. It has been reported that distribution of Fe^{3+} and Mn^{3+} ions is not homogeneous in such double-perovskite structures due to the very close ionic radii of Mn^{3+} and Fe^{3+}.[18] As a result, Fe-rich and Mn-rich clusters will form. Again, the Goodenough–Kanamori rules show that Fe–O–Fe in TMO_6 octahedra, where TM is a transition metal, will be ordered antiferromagnetically through 180° superexchange coupling. A strong AFM e_g^2-O-e_g^2 (Fe–O–Fe) interaction is favored by virtual charge transfer due to the two half-filled e_g orbitals of *HS* Fe^{3+}. For Mn–O–Mn, it can order antiferromagnetically through empty dz^2 to dz^2 and dx^2-y^2 to dx^2-y^2 orbits interactions both via oxygen $2p$ orbital and order ferromagnetically through superexchange mechanism between Mn half-filled dz^2 and empty dx^2-y^2 orbitals via oxygen $2p$ orbital in case of orbit ordering in $BiMnO_3$.[14] However, no evidence of orbital ordering can be found in the present data. Furthermore, based on the small magnetic moment observed in M-H loop, we conclude that Mn–O–Mn is antiferromagnetic ordered in Bi_2FeMnO_6. Because only one unpaired electron occupies the e_g orbital, Mn–O–Mn (e_g^1-O-e_g^1) ordering is much weaker than Fe–O–Fe ordering. Hence, the temperature of Fe–O–Fe ordering will be higher than that of Mn–O–Mn ordering. Based on the above reasons, the origins for the magnetic transitions at temperatures of 440 K, 260 K, and 150 K are attributed to Fe–O–Fe, Mn–O–Mn, and Fe–O–Mn orderings, respectively.

To further confirm the above analysis, magnetization (M) as a function of magnetic field (H) was measured at various temperatures. At 300 K, an unsaturated hysteresis loop with coercive field of 118 Oe is observed with AFM and FM components in a magnetic field of 1 kOe, as shown in

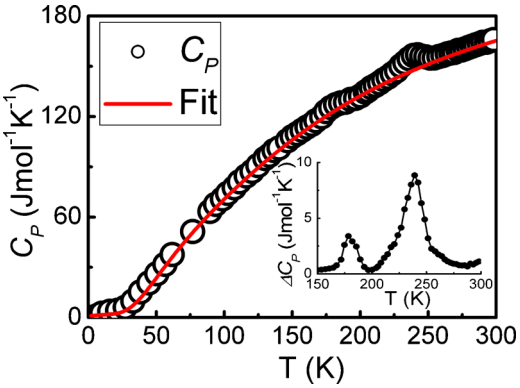

FIG. 3. (Color online) Heat capacity as a function of temperature from 2 to 300 K (symbols show the experimental data, and solid line is the fit). The inset is the excess magnetic heat capacity extracted from the total heat capacity by subtracting a smooth background using Debye–Einstein fitting.

the Fig. 2(b) inset. The magnetization is estimated to be 0.42 μ_B/f.u. at 1 kOe. The FM component is possibly attributable to a canted Fe moment arrangement. At 200 K, hysteresis behavior still remains in the *M-H* curve, with a coercive field of 82 Oe. However, the total behavior of *M-H* is dominated by a significant AFM contribution. At 5 K, a clear hysteresis loop with coercive field of 330 Oe and much reduced linear behavior is observed. The magnetic moment is estimated to be 4.48 μ_B/f.u. at 10 kOe, which is much smaller than the theoretical value of 9 μ_B/f.u. if all Fe^{3+} and Mn^{3+} ions are ordered ferromagnetically on the $B(B')$-site. Therefore, the magnetic transition at T_3 attributes to Fe–Mn ferrimagnetic ordering transition due to the small magnetic moment of the materials at low temperature.

The temperature dependence ($2\ \mathrm{K} < T < 300\ \mathrm{K}$) of the zero magnetic field heat capacity, C_p, is shown in Fig. 3 for Bi_2FeMnO_6. The overall shape of $C_p(T)$ follows the Dulong–Petit law, that is, the high temperature limiting value is consistent with the classical value of $3R$ per atomic site in the formula unit, where R is the molar gas constant. There are two clear λ-shaped anomaly peaks with peak temperatures of 242 and 175 K in the $C_p(T)$ curve, corresponding to the magnetic transitions at T_2 and T_3. Since no nonmagnetic analogs are available for this compound, the nonmagnetic contribution can be calculated by a combination of Debye and Einstein equations,[20]

$$C_p^{nm} = Nk_B\left\{\frac{9}{1-\eta_D T}\left(\frac{T}{\theta_D}\right)^3\int_0^{\theta_D/T}\frac{x^2\exp(x)}{[\exp(x)-1]^2}dx + \sum_{i=1}^{n}\frac{1}{1-\eta_E T}\frac{(\theta_{Ei}/T)^2\exp(\theta_{Ei}/T)}{[\exp(\theta_{Ei}/T)-1]^2}\right\}, \quad (1)$$

where η_D and η_E are the respective Debye and Einstein anharmonicity coefficients, θ_D is the Debye temperature, θ_E is the Einstein temperature, k_B is the Boltzmann constant, and N is mole number of the sample. The best fit was obtained by using two Einstein terms with an equivalent value for η_D and η_E. The fit is plotted in Fig. 3 as a solid line, which is in good agreement with the experimental data in the high temperature range. The parameters with the best fit were found to be $\eta_D = 0.0011\ \mathrm{K}^{-1}$, $\eta_E = 0.0011\ \mathrm{K}^{-1}$, $\theta_D = 339$ K, $\theta_{E1} = 255$ K, and $\theta_{E2} = 613$ K. The Debye temperature is comparable with those obtained for $BiFeO_3$ (340 K) and $BiMnO_3$ (290 K),[21–23] indicating the similar thermodynamic properties of these compounds. The magnetic contribution to the heat capacity, $\Delta C_p(T)$, therefore can be obtained by subtracting the nonmagnetic contribution from $C_p(T)$, as shown in the Fig. 3 inset. The high and broad peak at T_2 reflects the AFM Mn–O–Mn interaction. The peak at 175 K is associated with ferrimagnetic Fe–Mn ordering. Furthermore, the observation of this peak excludes its origin from spin-glass behavior, which has been observed in other materials with competition between different magnetic orderings.

In conclusion, Bi_2FeMnO_6 with double-perovskite structure was synthesized by an electrospray method. Magnetic measurements show the existence of Mn-rich and Fe-rich clusters. Although the fabrication method, starting from a solution precursor with an atomic-level Mn and Fe homogeneous distribution, was expected to result in Bi_2FeMnO_6 with homogeneous distribution of Mn and Fe, Mn-rich or Fe-rich clusters still appear due to their very close ionic radii and same charges. Therefore, it might be impossible to realize a one-by-one atomic arrangement of Mn and Fe in this material.

The authors thank the ARC for support through a Discovery Project and a Future Fellowship. Y. Du thanks Dr. Z. P. Guo and Mr. P. Zhang for help in using the electrospray system.

[1] B. K. Ponomarev, S. A. Ivanov, Y. F. Popov, V. D. Negrii, and B. S. Red'kin, Ferroelectrics **161**, 43 (1994).
[2] H. Schmid, Ferroelectrics **162**, 317 (1994).
[3] N. A. Hill, J. Phys. Chem. B **104**, 6694 (2000).
[4] M. Gajek, M. Bibes, A. Barthélémy, K. Bouzehouane, S. Fusil, M. Varela, J. Fontcuberta, and A. Fert, Phys. Rev. B **72**, 020406(R) (2005).
[5] Z. X. Cheng, X. L. Wang, S. X. Dou, K. Ozawa, and H. Kimura, Phys. Rev. B **77**, 092101 (2008).
[6] J. B. Neaton, C. Ederer, U. V. Waghmare, N. A. Spaldin, and K. M. Rabe, Phys. Rev. B **71**, 014113 (2005).
[7] J. Wang, J. B. Neaton, H. Zheng, V. Nagarajan, B. Ogale, B. Liu, D. Viehland, V. Vaithyanathan, D. G. Schlom, U. V. Waghmare, N. A. Spaldin, K. M. Rabe, M. Wuttig, and R. Ramesh, Science **299**, 1719 (2003).
[8] Z. X. Cheng, X. L. Wang, H. Kimura, K. Ozawa, and S. X. Dou, Appl. Phys. Lett. **92**, 092902 (2008).
[9] Y. Chu, Q. He, C. Yang, P. Yu, L. W. Martin, P. Shafer, and R. Ramesh, Nano Lett. **9**, 1726 (2009).
[10] R. Schmidt, W. Eerenstein, and P. A. Midgley, Phys. Rev. B **79**, 214107 (2009).
[11] T. Kimura, S. Kawamoto, I. Yamada, M. Azuma, M. Takano, and Y. Tokura, Phys. Rev. B **67**, 180401(R) (2003).
[12] R. Schmidt, W. Eerenstein, T. Winiecki, F. D. Morrison, and P. A. Midgley, Phys. Rev. B **75**, 245111 (2007).
[13] Y. Tokunaga, S. Iguchi, T. Arima, and Y. Tokura, Phys. Rev. Lett. **101**, 097205 (2008).
[14] L. Bi, A. R. Taussig, H. Kim, L. Wang, G. F. Dionne, D. Bono, K. Persson, G. D. Ceder, and C. A. Ross, Phys. Rev. B **78**, 104106 (2008).
[15] H. Zhao, H. Kimura, Z. Cheng, X. Wang, and T. Nishida, Appl. Phys. Lett. **95**, 232904 (2009).
[16] J. B. Goodenough, A. Wold, R. J. Arnott, and N. Menyuk, Phys. Rev. **124**, 373 (1961).
[17] W. Bao, J. D. Axe, C. H. Chen, and S. Cheong, Phys. Rev. Lett. **78**, 543 (1997).
[18] W. Tong, B. Zhang, S. Tan, and Y. Zhang, Phys. Rev. B **70**, 014422 (2004).
[19] J. B. Goodenough, *Magnetism and the Chemical Bond* (Wiley, New York, 1963).
[20] C. A. Martin, J. Phys.: Condens. Matter **3**, 5967 (1991).
[21] C. Blaauw and F. van der Woude, J. Phys. C **6**, 1422 (1973).
[22] A. A. Belik and E. Takayama-Muromachi, Inorg. Chem. **45**, 10224 (2006).
[23] See supplementary material at http://dx.doi.org/10.1063/1.3490221 for SEM, XPS, and EDS mapping results.